

A solution thermodynamics definition of the fiber saturation point and the derivation of a wood–water phase (state) diagram

Samuel L. Zelinka¹  · Samuel V. Glass¹ ·
Joseph E. Jakes² · Donald S. Stone³

Received: 16 April 2015 / Published online: 10 December 2015
© Springer-Verlag Berlin Heidelberg (outside the USA) 2015

Abstract The fiber saturation point (FSP) is an important concept in wood–moisture relations that differentiates between the states of water in wood and has been discussed in the literature for over 100 years. Despite its importance and extensive study, the exact theoretical definition of the FSP and the operational definition (the correct way to measure the FSP) are still debated because different methods give a wide range of values. In this paper, a theoretical definition of the FSP is presented based on solution thermodynamics that treats the FSP as a phase boundary. This thermodynamic interpretation allows FSP to be calculated from the chemical potentials of bound and free water as a function of moisture content, assuming that they are both known. Treating FSP as a phase boundary naturally lends itself to the construction of a phase diagram of water in wood. A preliminary phase diagram is constructed with previously published data, and the phase diagram is extended to a state diagram by adding data on the glass transition temperatures of the wood components. The thermodynamic interpretation and resulting state diagram represent a potential framework for understanding how wood modification may affect wood–moisture relations.

✉ Samuel L. Zelinka
szelinka@fs.fed.us

¹ Building and Fire Sciences, US Forest Service, Forest Products Laboratory, 1 Gifford Pinchot Drive, Madison, WI 53726, USA

² Forest Biopolymers Science and Engineering, US Forest Service, Forest Products Laboratory, 1 Gifford Pinchot Drive, Madison, WI 53726, USA

³ Materials Science and Engineering, University of Wisconsin, Madison, 1509 University Ave, Madison, WI 53706, USA

Introduction

Wood is a hygroscopic material that freely exchanges moisture with the environment and retains moisture in its various phases: water vapor, liquid water, or ice within voids and bound (adsorbed) water within the cell wall. The amount of moisture in wood is described by wood moisture content (MC), calculated by

$$MC = \frac{m_{\text{water}}}{m_{\text{wood}}} \quad (1)$$

where m_{water} is the mass of water in the wood and m_{wood} is the dry mass of the wood itself. Although normally presented as a fraction (kg kg^{-1}) or percentage, moisture content is not the same as the mass fraction of water and moisture contents of over 100 % are possible.

The physical and mechanical properties of wood are strongly dependent on moisture content. While wood has served as a versatile building material for several millennia and continues to be used successfully, many of the practical difficulties with its use, such as dimensional instability, microbial attack, and fastener corrosion, are caused by the interaction or abundance of moisture in wood. Understanding wood–moisture interactions is necessary for developing modifications and treatments to protect wood from these damage mechanisms as well as ensuring the durability and sustainability of wood structures.

Despite the important effects of moisture on wood properties, there are differences in the literature about how water interacts with wood and where it is stored. In general, it is believed moisture in wood can be held by the wood polymers or occupy empty space within the cellular structure. Traditionally, these are referred to as “bound water” and “free water,” respectively. The *fiber saturation point*, often called FSP, is a concept used to differentiate between the two. In simple terms, FSP is the moisture content below which there is only bound water. Above the fiber saturation point, both bound water and free water exist. While FSP is conceptually simple, there are many ways to measure FSP, resulting in a wide range of reported values of the FSP (between roughly 30 and 40 % MC) and debate about which method is the most accurate (Stamm 1971; Skaar 1988).

The fiber saturation point was originally defined by Tiemann (1906) and came from observations of the ultimate crushing strength of wood at different moisture contents. Tiemann observed that as specimens were dried from the green state, no difference in crushing strength was observed until they reached a certain moisture content at which the crushing strength increased parabolically. Tiemann assigned the words “fiber saturation point” to the intersection of these two curves and gave it the following theoretical definition:

“In drying out a piece of wet wood, since the free water must evidently evaporate before the absorbed moisture in the cell walls can begin to dry out, there will be a period during which the strength remains constant although varying degrees of moisture are indicated. But just as soon as the free water has disappeared and the cell walls begin to dry the strength will begin to increase. This point I designate the fiber-saturation point.”

Siau (1995) paraphrases Tiemann's definition as "the moisture content at which the cell wall is saturated while the voids are empty." Skaar (1988) interprets Tiemann's statement as the moisture content at which "cell cavities contained no liquid water, but the cell walls were fully saturated with moisture." While there are slight differences between the definitions, in the most general terms, they all refer to a moisture content at which the cell wall can accommodate no more moisture and above which a second phase (liquid water) is present in voids.

While the theoretical definition of the fiber saturation point is associated with a clear physical picture, there has been little consensus on how to measure the fiber saturation point. Both Stamm (1971) and Skaar (1988) have reviewed methods used to measure the fiber saturation point and list nine and ten different methods, respectively. In essence, each method for determining the fiber saturation point is, in a way, a different *operational definition* as each method gives different values for the fiber saturation point.

First, theoretical and operational definitions of the fiber saturation point are briefly reviewed before presenting a thermodynamics framework for defining the fiber saturation point. It will be shown that this definition does not easily lend itself to an operational method to measure the FSP. Despite this, the thermodynamics definition of the FSP lends itself to the construction of a phase or state diagram for water in wood. Based upon the thermodynamics definition and published data, a phase diagram for wood is constructed.

Ways to measure FSP and implied operational definitions

A variety of techniques have been used to measure the fiber saturation point in wood (Stamm 1971; Skaar 1988). Depending on the method used and the wood species, the reported values of the fiber saturation point range from less than 20 % MC to higher than 40 % MC. Ignoring species with high extractives content, typical values are roughly 30–40 % MC depending on method. Clearly, these different measurement techniques affect the measured FSP because of the inherent assumptions of how the measurement technique relates to theoretical definition of FSP. Here, different methods used to measure FSP are briefly reviewed, highlighting their inherent assumptions so that they can be compared to the theoretical definition of FSP.

Changes in physical properties

Beginning with the original experiments by Tiemann (1906), FSP has often been measured by examining a physical or mechanical property for a discontinuity (first-order transition) or a discontinuity in the derivative (second-order transition). Wood physical properties that exhibit a first- or second-order transition include strength (Tiemann 1906), shrinkage (Stamm 1935), and electrical conductivity (Stamm 1929; James 1963, 1988). These methods predict a fiber saturation point of roughly 30 % moisture content (Stamm 1971).

For “practical purposes” such as using wood as a construction material, these methods are well suited for determining the fiber saturation because they directly measure whether or not a critical parameter relevant to the structural performance is changing with moisture content. These methods are simple, are inexpensive, and represent a good practical limit for the change in wood properties with moisture. However, they are not necessarily related to the theoretical definition of the fiber saturation point. While changes in the macroscopic physical properties are certainly related to moisture-induced changes in the cell wall, their behavior may not necessarily change at the same moisture content at which the cell walls can no longer accommodate moisture. For example, FSP is calculated from the intersection of two tangent lines from a graph of the conductivity versus moisture content (Stamm 1971). While this is useful in determining the point of a slope change in the conductivity, it is unclear how this slope change is related to how moisture is partitioned in the cell wall.

Differential scanning calorimetry

A closely related measurement technique involves differential scanning calorimetry (DSC) (Deodhar and Luner 1980; Nakamura et al. 1981; Simpson and Barton 1991; Weise et al. 1996; Hatakeyama and Hatakeyama 1998; Kärenlampi et al. 2005; Repellin and Guyonnet 2005; Miki et al. 2012; Zelinka et al. 2012; Zauer et al. 2014). In these measurements, samples are prepared over a range of moisture contents. Heat flux is measured, while the temperature is scanned at a certain rate below and above the water freezing point. The freezing/melting peak of water is only observed at moisture contents where there is free water. Alternatively, FSP can be calculated from measuring the melting enthalpy of water-saturated samples and dividing it by the heat of fusion of pure water to find the mass of water that froze. The reported FSPs determined from DSC range from as low as 25 % MC to as high as 40 % MC. This technique measures the maximum amount of water that wood cell walls can hold before a second phase is formed and is therefore very close to the theoretical definition; however, it requires extrapolation and is limited by the accuracy of the measurement since there needs to be enough free water freezing to generate a signal. The method is also affected by the scan rate, since kinetic supercooling can mask the phase transitions at the scan rates typically used to measure freezing of water in wood (Landry 2005). The method is also limited to the melting temperature; it cannot measure FSP at room temperature, for example.

Nuclear magnetic resonance

Researchers have used nuclear magnetic resonance (NMR) and, similarly, magnetic resonance imaging (MRI) to examine the states of water in wood (Menon et al. 1987; Araujo et al. 1992; Almeida et al. 2007; Hernández and Cáceres 2010; Telkki et al. 2013; Passarini et al. 2014, 2015; Lamason et al. 2015). In these measurements, a magnetic pulse is applied and the transverse relaxation time (T_2) of water can be measured. The speed of T_2 relaxation time is dependent on whether the water is bound or unbound and can also depend upon the size of the unbound

water domains (Telkki 2012). Bound water has a very short relaxation time (<1 ms), and free water in large cell cavities such as vessel elements in hardwoods or tracheid lumina in softwoods can have relaxation times of the order of hundreds of milliseconds (Almeida et al. 2007). An intermediate T_2 relaxation time (between 1 and 20 ms) is attributed to water in small pores in the wood structure (Almeida et al. 2007). Telkki et al. (2013) used NMR to determine the FSP by measuring relaxation times above and below 0 °C. Below 0 °C, the free water relaxation time was not visible, and the comparison between the measurements above and below the water melting point allowed the determination of the FSP. Telkki et al. (2013) report a FSP of 35 % for pine (*Pinus sylvestris*) and 45 % for spruce (*Picea abies*). Several researchers have qualitatively examined T_2 times as a function of wood moisture content in hardwoods. They have observed water with medium relaxation times in wood that had been conditioned at moisture contents as low as 16 % MC (Almeida et al. 2007). Both NMR and DSC measurements appear to have great promise in determining FSP since they are able to quantitatively examine the amount of water in different states within wood; however, both techniques have a large range of reported FSPs.

Solute exclusion method

The “polymer exclusion method” or “non-solvent water” technique is another method used to measure the fiber saturation point. In this method, water-saturated wood is placed into a dilute solution (Feist and Tarkow 1967; Stone and Scallan 1967; Flournoy et al. 1991, 1993; Hill et al. 2005). A range of differently sized molecules is used to probe the nano- and mesoscale porosity. After the wood has been in the solution for a long time, the concentration in the external solution is measured. This concentration is lower than the original concentration because the accessible pores in the wood diluted the solution, which allows the accessible volume to be calculated. For large probes, the accessible volume is independent of probe size, and this accessible volume is due to the water in the lumina and other large openings in the cell wall. FSP can be calculated by the difference in accessible volume between the smallest probe (a water molecule) and this plateau (Hill et al. 2005). This technique is frequently cited as the most natural or correct way to measure FSP since it is a measure of the water that is interacting with the wood (Hill 2008; Hoffmeyer et al. 2011; Engelund et al. 2013). Bound or entrapped water in the solute exclusion method cannot dilute the polymer solution, whereas free water can. However, this method assumes that the polymer solution can infiltrate all of the voids where free water exists. The polymer exclusion technique predicts a much higher FSP (roughly 40 %) than those methods that measure discontinuities in physical properties (Stamm 1971; Engelund et al. 2013).

Pressure plate technique

The pressure plate technique (PPT) is a way to measure the equilibrium moisture content (EMC) in wood when the relative humidity (RH) is very high. Strictly speaking, relative humidity is equivalent to the activity of water a_w , i.e.,

$$\text{RH} \equiv a_w = p_{\text{H}_2\text{O}}/p_{\text{H}_2\text{O}}^0 \quad (2)$$

where $p_{\text{H}_2\text{O}}$ and $p_{\text{H}_2\text{O}}^0$ are the vapor pressure and the saturated vapor pressure of water, respectively. Because it is very difficult to fix the vapor pressure of water near its saturation point, the pressure plate technique controls the activity of water by applying an external pressure. In this technique, wood that is fully saturated with water is placed on a porous ceramic plate and the pressure on one side of the wood is increased to as much as 1.5–2 MPa; if a membrane is used rather than a ceramic plate, the pressure can be increased up to 10 MPa. A similar technique uses a centrifuge to apply the external pressure (Choong and Tesoro 1989). In both cases, the applied pressure fixes the activity of water; the applied pressure is opposed by capillary forces that retain water depending on the pore size. The Kelvin equation relates the water activity to a radius of curvature of the air–water interface, r_{lg} (m):

$$r_{\text{lg}} = \frac{-2\sigma_{\text{lg}}V_m}{RT \ln a_w} \quad (3)$$

where σ_{lg} is the surface tension of water (0.07199 N m⁻¹ at 25 °C), V_m is the molar volume of water (1.806 × 10⁻⁵ m³ mol⁻¹ at 25 °C), R is the universal gas constant (8.314 J mol⁻¹ K⁻¹), and T is the absolute temperature (K). With the assumption of cylindrical pores, the pore radius r_p (m) can be related to the radius of curvature r_{lg} and the contact angle θ through $r_p = r_{\text{lg}} \cos \theta$.

Stone and Scallan were the first researchers to use the pressure plate technique to calculate the fiber saturation point (Stone and Scallan 1967). They defined the fiber saturation point as EMC at $a_w = 0.9975$ (0.4 μm radius) because the relationship between moisture content and water activity had an inflection at that point. They argued that at this point, all of the cell wall pores are filled, but all of the lumina are empty. Griffin reanalyzed their data and argued that the inflection and fiber saturation point actually occur at 1 bar of applied pressure ($a_w = 0.9993$, 1.5 μm radius) (Griffin 1977).

The FSPs determined by pressure plate measurements are similar to those found by the solute exclusion method. In both techniques, FSP is defined by a cutoff pore size; water in pores smaller than the critical radius is considered bound water and water in larger pores is considered free water.

Extrapolation of the sorption isotherm

The extrapolation of the sorption isotherm is based upon a thermodynamic interpretation of the fiber saturation point. A sorption isotherm is the locus of points relating the relative humidity to the moisture content of a material at equilibrium at a given temperature. Single-component condensed phases, such as liquid water, have an activity of unity. Therefore, researchers have extrapolated the sorption isotherm to 100 % relative humidity (i.e., $a_w = 1$) to predict the fiber saturation point (Stamm 1971; Berry and Roderick 2005).

From a theoretical standpoint, extrapolation to 100 % RH is not strictly correct, since the activity of the free (liquid) water will be less than unity because it is in the

presence of another phase (i.e., the wood). For example, if the free water phase in wood was assumed to be an ideal solution, it would follow Raoult's law and the activity would be proportional to mole fraction. Clearly, water in wood is not an ideal solution; however, it is important to note that even in the ideal solution limit, thermodynamics tells us that free water will be present at a relative humidity of less than 100 %.

While the extrapolation of the isotherm to 100 % relative humidity is not an accurate description of the fiber saturation point, conceptually, it is similar to the thermodynamic definition of the fiber saturation point which is now presented here.

Solution thermodynamics definition of the fiber saturation point

Here, solution thermodynamics is used to derive a theoretical definition of the fiber saturation point. To present the solution thermodynamics model, it is first necessary to clarify the definition of a *phase* and *component*. A *phase* refers to a volume of material in which the properties, both chemical and physical, are uniform. A *component* is a chemical species of fixed composition, for example pure tin, or a mixture of 50 wt% lead and 50 wt% tin. For example, in the two-component lead–tin system, lead has a face-centered cubic (FCC) crystal structure and tin has a tetragonal crystal structure. Lead can accommodate some tin atoms within the FCC structure. However, as the amount of tin increases, the alloy can no longer accommodate all of the tin atoms into the FCC structure and a two-phase solid (FCC, rich in lead, and tetragonal, rich in tin) forms. The maximum amount of tin that lead can accommodate within the FCC structure is called the phase boundary.

To define the fiber saturation point, solid wood is treated as a single phase that can accommodate water within its molecular structure below the fiber saturation point (which is the phase boundary). Liquid water and water vapor are other key phases in this system. The model here treats wood as a single component. While the chemical composition of wood varies from species to species, from tree to tree, and even with location from within a given tree, for the purposes of water adsorption it can be treated as a single component because (1) when water is added to it, the composition does not change and (2) for a given block of wood that is adsorbing water, the composition is nearly uniform. Furthermore, certain wood constituents, such as crystalline cellulose, may be an inert, elastic scaffold around which the wood–moisture interactions take place. Water is clearly a single component, and therefore, this thermodynamic system has two components.

Previous theoretical definitions of the fiber saturation point from Skaar (1988) and Siau (1995) can be interpreted in terms of a phase boundary. A phase boundary at a given temperature and pressure is the maximum amount of a component that can be accommodated into a phase before a new phase forms. In this case, FSP represents the maximum amount of water the wood phase can accommodate before a new phase (liquid water) appears. In thermodynamics, phase boundaries can be determined from the chemical potential of each phase. At a phase boundary, the chemical potential of each component must be equal in both phases because they are in equilibrium. Therefore, the fiber saturation point can be defined by

$$\mu_{\text{H}_2\text{O}}^{\text{bound}} = \mu_{\text{H}_2\text{O}}^{\text{free}} \quad (\text{at FSP}) \quad (4)$$

where $\mu_{\text{H}_2\text{O}}^{\text{bound}}$ (J mol^{-1}) is the chemical potential of bound water and $\mu_{\text{H}_2\text{O}}^{\text{free}}$ (J mol^{-1}) is the chemical potential of free water. Now that the fiber saturation point has been defined, expressions need to be found that relate the chemical potential of bound and free water to the wood moisture content.

The chemical potential of free water as a function of wood moisture content can be determined by pressure plate measurements or mercury intrusion porosimetry (MIP) measurements. The chemical potential of liquid water in small capillaries is affected by surface tension and the interaction with the solid surface and is therefore different from the chemical potential of bulk water. The chemical potential of liquid water in a pore can be determined from

$$\mu_{\text{H}_2\text{O}}^{\text{free}} = -p_c V_m \quad (5)$$

where p_c is the capillary pressure (Pa), the negative of the applied pressure in a PPT experiment, and V_m is the molar volume of water ($1.806 \times 10^{-5} \text{ m}^3 \text{ mol}^{-1}$ at $25 \text{ }^\circ\text{C}$). Capillary pressure can also be related to mercury pressure in a MIP experiment as described in the following section.

Determining the chemical potential of bound water as a function of moisture content is less straightforward. Le Maguer (1985) presented a method for calculating the chemical potential of water as a function of moisture content for hydrophilic polymers from the sorption isotherm. Because the sorption isotherm is a collection of equilibrium measurements, at each point along the isotherm, the chemical potential of the water in the wood must be equal to the chemical potential of water in the vapor phase, or equivalently

$$\mu_{\text{H}_2\text{O}}^{\text{bound}} = RT \ln(a_w) = RT \ln(\text{RH}) \quad (6)$$

This calculation of $\mu_{\text{H}_2\text{O}}^{\text{bound}}$ implicitly assumes that the sorption isotherm contains only bound water. If the sorption isotherm corresponds only to bound water, then FSP can be determined graphically by plotting the chemical potential of water, calculated from Eqs. 5 and 6 as a function of wood moisture content. The intersection of these curves is the moisture content at which the chemical potential of bound water is equal to the chemical potential of free water, which represents a phase boundary, and the thermodynamic fiber saturation point. This construction is now illustrated from measurements of southern pine (*Pinus spp.*).

Methods

Here, it is illustrated how the solution thermodynamics framework can be used to calculate FSP using data from previous measurements of the moisture retention curve of southern pine (*Pinus spp.*) (Zelinka et al. 2014). However, the framework can be used for any measurements of the chemical potential of bound and free water

and is not limited to the MIP and sorption data presented. The wood was harvested from a plantation where over 90 % of the trees were slash pine (*Pinus elliottii*). The chemical potential of the free water in pores was determined from mercury intrusion porosimetry measurements, and the chemical potential of water at low water activities was determined from the sorption isotherm.

The MIP measurements were performed using 300- μm -thick microtomed transverse sections so that on average the lumina were accessible from at least one side (Trenard 1980). The measurements were taken on a PoreMaster 60 GT porosimeter (Quantachrome Instruments, Boynton Beach, FL) over a pressure range of 1.4 kPa to 410 MPa. The raw data were the volume of mercury intruded as a function of the mercury pressure and were transformed into the wood moisture content as a function of capillary pressure. Capillary pressure is related to the chemical potential of water by Eq. 5. The capillary pressure of water was calculated from the mercury pressure P_{Hg} (Pa) through

$$p_c = -P_{\text{Hg}} \frac{\sigma_w \cos \theta_w}{\sigma_{\text{Hg}} \cos \theta_{\text{Hg}}} \quad (7)$$

where σ_w is the surface tension of water (0.07199 N m^{-1} at $25 \text{ }^\circ\text{C}$), σ_{Hg} is the surface tension of mercury (485.5 N m^{-1} at $25 \text{ }^\circ\text{C}$), θ_w is the contact angle of water, and θ_{Hg} is the contact angle of mercury. The commonly assumed values of 0° (perfectly wetting) and 130° were used for the contact angles of water and mercury, respectively. The wood moisture content was calculated from MIP measurements as follows. The total moisture content (kg of moisture per kg of dry wood) above the fiber saturation point was taken as the sum of bound water content and free water content:

$$\text{MC} = \text{MC}_{\text{bound}} + \text{MC}_{\text{free}} \quad (8)$$

The free water content was calculated from the mercury intrusion data:

$$\text{MC}_{\text{free}} = \rho_l \left(v_{\text{Hg}}^{\text{max}} - v_{\text{Hg}} \right) \quad (9)$$

where ρ_l is the density of water (997 kg m^{-3} at $25 \text{ }^\circ\text{C}$), v_{Hg} is the specific volume of mercury (m^3 of Hg per kg of dry wood) intruded at a given applied pressure, and $v_{\text{Hg}}^{\text{max}}$ is the maximum specific volume of mercury, taken as $1.285 \text{ cm}^3 \text{ g}^{-1}$, which occurs from about 10 MPa to about 200 MP and corresponds with filling of macrovoids.

At total saturation, Eq. 8 can be used to calculate the bound water content (above the fiber saturation point) from the difference between the moisture content at total saturation and the maximum free water content:

$$\text{MC}_{\text{sat}} = \text{MC}_{\text{bound}} + \text{MC}_{\text{free}}^{\text{max}} = \text{MC}_{\text{bound}} + \rho_l v_{\text{Hg}}^{\text{max}} \quad (10)$$

Combining Eqs. 8–10 yields the wood moisture content as a function of specific volume of mercury:

$$\text{MC} = \text{MC}_{\text{sat}} - \rho_l v_{\text{Hg}} \quad (11)$$

Moisture content at saturation of the MIP specimen was calculated as $MC_{\text{sat}} = 1/G_b - 1/G_{\text{cw}}$, where G_b is the basic specific gravity (dry mass, swollen volume) and G_{cw} is the cell wall specific gravity (Glass and Zelinka 2010). The apparent cell wall specific gravity determined by the MIP experiment was 1.355; this value is considerably less than commonly obtained values of 1.5–1.6, and the influence is discussed below. Because the basic specific gravity of the MIP specimen could not be directly measured, it was estimated using the dry specific gravity (0.494) determined by the MIP experiment and separate measurements of saturated moisture content in 16 replicates of 25-mm cube specimens from the same parent board of southern pine. These measurements showed good correlation ($R^2 = 0.89$) between MC_{sat} and basic specific gravity and between MC_{sat} and oven-dry specific gravity. The basic specific gravity of the MIP specimen was estimated from these correlations to be 0.438. MC_{sat} of the MIP specimen was thus calculated to be 1.544 kg kg⁻¹. As mentioned above, this value relies on the apparent cell wall specific gravity determined by the MIP experiment; a value of $MC_{\text{sat}} = 1.633$ kg kg⁻¹ is obtained (difference of 9 % MC) using a cell wall specific gravity of 1.54 rather than 1.355.

The desorption isotherm was collected on 300- μm -thick cross sections with an IGAsorp gravimetric vapor sorption analyzer (Hiden Isochema, Warrington, UK). Immediately prior to testing, samples were immersed in water until they sank and then held underwater for 24 h; the small sample size along the transverse section made air entrapment unlikely. The sample was then suspended from a microbalance (resolution of 0.1 μg) in a temperature-controlled chamber through which flowed a nitrogen stream with controlled humidity, generated by mixing dry and saturated nitrogen streams using electronic mass flow controllers. Measurements were taken at 25 °C at the following relative humidity conditions in desorption from a water-saturated condition: 95, 92.5, 90–5 % in increments of 5%, and 2.5 %. For each condition, the sample was exposed for at least 20 h. In some cases (high RH), the sample was exposed for as long as 90 h. The percent change in relative mass at the end of the conditioning period was between 10 and 110 ppm/h (0.00002–0.0002 % per minute). The equilibrium mass at each step was determined by extrapolation of a single exponential curve fit to the time-dependent mass response following a step change in RH. The dry mass of the sample was measured after all the data had been collected, under flow of dry nitrogen with the sample temperature brought to 105 °C. Assuming that the sample did not contain significant volatile compounds other than water, moisture content determinations with this method have a measurement error of approximately ± 0.001 kg kg⁻¹.

The sorption isotherm data were analyzed in the manner of Le Maguer where the chemical potential of water was calculated from Eq. 6 and plotted as a function of moisture content. This was compared to the chemical potential/moisture content data from the MIP experiment to determine the FSP.

Results and discussion

FSP determined from MIP and sorption isotherm measurements

The specific volume of mercury from MIP measurements is plotted versus mercury pressure in Fig. 1. The sorption isotherm data are plotted in the customary way as EMC versus RH in Fig. 2 and are fit with a curve described below. The two sets of data are combined using the calculation methods above to give the chemical potential of water as a function of the wood moisture content in Fig. 3, assuming that the sorption isotherm represents only bound water. The two sets of data do not directly intersect, but given the shape of the curves, it is clear that the chemical potential of free water will intersect that of bound water at a moisture content of approximately 0.26 kg kg^{-1} and a chemical potential of approximately -80 J mol^{-1} . To arrive at a better estimation of the phase boundary, the sorption isotherm is extrapolated by fitting the data to the following function used to describe water vapor sorption isotherms in wood:

$$\frac{a_w}{MC} = A(a_w)^2 + B(a_w) + C \quad (12)$$

where A , B , and C are fitting parameters (Zelinka and Glass 2010). This equation is mathematically equivalent to the Hailwood and Horrobin (1946), Dent (1977), and GAB isotherms (Anderson 1946). This fitting curve is shown in Figs. 2 and 3 (where it has been transformed using the relation between water activity and chemical potential given in Eq. 6). Through this extrapolation, and the assumption that the isotherm only contains bound water, one arrives at a value of the fiber saturation point of 0.263 kg kg^{-1} and a chemical potential of approximately -83 J mol^{-1} ($a_w = 0.967$). It should be noted that the absolute value of this FSP is

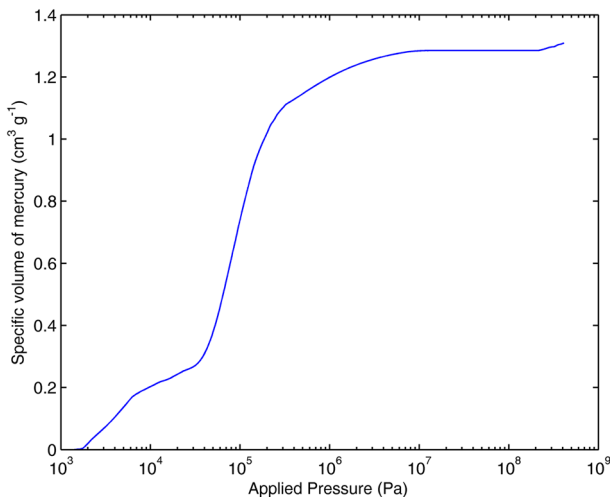


Fig. 1 Specific volume of intruded mercury versus applied pressure from MIP measurements

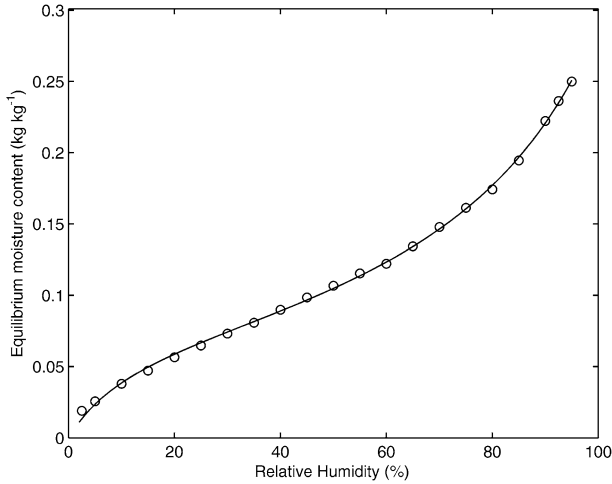


Fig. 2 Equilibrium moisture content versus relative humidity at 25 °C measured in desorption from water-saturated condition. Curve fit corresponds to Eq. 12

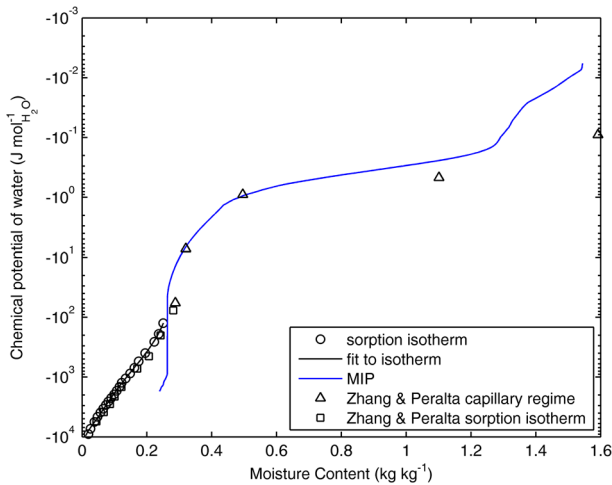


Fig. 3 Graphical method used to find the thermodynamic FSP. The chemical potential of free water is determined from MIP measurements. The chemical potential calculated from sorption isotherms is used as a bound water curve. The intersection represents the phase boundary between bound and free water. The data of Zhang and Peralta (1999) for loblolly pine are shown for comparison

affected by uncertainties in the MIP measurement; however, the framework presented in Fig. 3 can be applied to any two measurements of the chemical potential of bound and free water for a specific piece of wood.

The data of Zhang and Peralta (1999) for loblolly pine at 30 °C are also plotted in Fig. 3 for comparison. These data were obtained with the pressure plate and pressure membrane techniques and by conditioning specimens over saturated salt

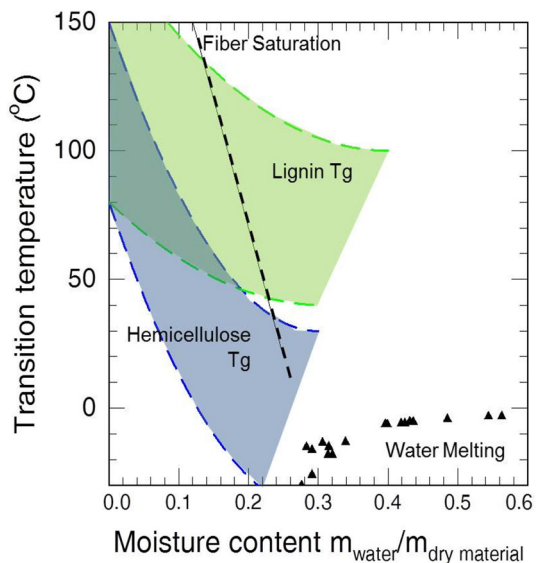
solutions in desorption. The pressure plate/pressure membrane measurements in the moisture content range between 0.25 and 0.50 kg kg⁻¹ are fairly close to the values calculated from the MIP measurements presented here. The sorption isotherm and pressure membrane data of Zhang and Peralta intersect at a moisture content between 0.281 and 0.288 kg kg⁻¹ and a chemical potential between -58 and -77 J mol⁻¹ ($0.970 \leq a_w \leq 0.977$).

Binary phase diagram for wood–water system

The thermodynamic definition of the fiber saturation point presented in this paper (i.e., $\mu_{\text{H}_2\text{O}}^{\text{bound}} = \mu_{\text{H}_2\text{O}}^{\text{free}}$ at FSP) can be calculated in terms of chemical potentials of bound water and free water, assuming that they are known, and treats FSP as a thermodynamic phase boundary. In defining FSP as a phase boundary, the next logical extension is the derivation of a phase diagram. For other hydrophilic natural materials, such as certain foods, phase diagrams are used to describe the changes in material with moisture content (Vuataz 2002). Often, the data are combined with glass transition temperature data to create “state diagrams” describing both the mechanics and thermodynamics (Roos and Karel 1991a, b).

A preliminary state diagram is shown in Fig. 4 for wood based upon the presented data of water phase transitions in wood and the range of published data on the mechanical properties of wood as a function of moisture content. The line labeled “Fiber Saturation” represents the temperature dependence of the fiber saturation point on temperature as described by Siau (1995) and also Skaar (1988), which is believed to be based on sorption isotherm data in the *Wood Handbook* (Glass and Zelinka 2010) that has recently come into question (Glass et al. 2014). The glass transition temperatures of the lignin and hemicelluloses come from

Fig. 4 Preliminary state diagram of water in wood constructed from literature data on the glass transitions of wood polymers and calorimetric studies on water in wood



several sources (Cousins 1976, 1978; Salmén and Olsson 1998; Olsson and Salmen 2004a, b); these data appear as broad regions on the phase diagram because of variations in the data. It should be noted that the data were collected on extracted lignin and hemicelluloses and some of the variation represented on the phase diagram represents uncertainty in what the actual glass transition temperatures are, in situ. In actuality, if FSP has been reached, the T_g should not change with increasing MC since the additional water would not be interacting with the polymers; the fact that these regions extend past the line labeled “Fiber Saturation” may be a result of the measurements being performed on isolated lignin and hemicellulose as well as the uncertainty in the data used to construct the “Fiber Saturation” line. The “Water Melting” curve in the phase diagram comes from differential scanning calorimetry (DSC) measurements of the freezing and melting of water in loblolly pine (Zelinka et al. 2012). In these experiments, a range of wood moisture contents was brought to $-65\text{ }^\circ\text{C}$ at $5\text{ }^\circ\text{C}$ per minute, held at $-65\text{ }^\circ\text{C}$ for 5 min, and brought up to $25\text{ }^\circ\text{C}$ at $5\text{ }^\circ\text{C}$ per minute. No melting peak was observed below FSP; above FSP, there was thermodynamic undercooling of the melting temperature, and the amount of undercooling was largest near the fiber saturation point and decreased as the moisture content increased.

The state diagram presented in Fig. 4 can be used to illustrate, both qualitatively and quantitatively, how water behaves in wood under different circumstances. Researchers have examined how chemical modification of wood affects the amount of bound water that wood can hold (e.g., Hill 2008; Thygesen and Elder 2008, 2009; Thygesen et al. 2010). The reduction in water retention has been attributed to changes in the sorption sites, such as micropore blocking and/or binding of the modification compounds to sorption sites. By using a state diagram, it is also possible to explore the interrelationship between mechanical property changes caused by chemical modification and changes in FSP. Several researchers have hypothesized that the sorption process is related to and possibly limited by the glass transitions of the hemicelluloses in wood (Engelund et al. 2013; Jakes et al. 2013). By constructing state diagrams for modified wood, it is possible to further explore this relationship. For example, if a chemical modification raised the glass transition temperature of the hemicelluloses and lowered FSP, it suggests that moisture content in these systems is limited by the softening of the hemicelluloses and gives a thermodynamic mechanism by which the chemical modification lowers the amount of water that wood can hold at a given water activity.

The state diagram can also be used to explore the interaction of free water with the wood. In contrast to sorption theories that assume a certain number of sorption sites in the wood and break down above the fiber saturation point when free water forms, the framework presented in this paper can account for the thermodynamics of water in wood both above and below FSP (defined as a phase boundary). The intersection of the “Fiber Saturation” and DSC data on the state diagram is analogous to a eutectic phase transformation frequently found in mixtures of inorganic compounds. In a eutectic phase transformation, the first liquid forms at a temperature lower than the melting temperature of any of the pure components. For example, the lead–tin system used in solders has a eutectic temperature of $183\text{ }^\circ\text{C}$, compared with the melting point of $327\text{ }^\circ\text{C}$ for pure lead or $232\text{ }^\circ\text{C}$ of pure tin. In

the food sciences, where freeze-drying is an important preservation method, eutectic phase transformations are frequently reported (Vuataz 2002; Gliguem et al. 2009), including carbohydrate–water systems such as glucose, which are chemically similar to wood components (Roos and Karel 1991a, b). While not completely unexpected, this apparent eutectic-like behavior in the wood–moisture system may give clues to how and where the free water forms in wood if the eutectic phase transformation happens the same in wood as it does for inorganic compounds.

Limitations of the solution thermodynamics definition

While the solution thermodynamics definition of FSP and the wood–water state diagram provide new insight, the analysis rests on several assumptions and simplifications.

First, viewing the fiber saturation point as a phase boundary and constructing a binary phase diagram rely on the assumption that wood is a single component. Cellulose, hemicelluloses, lignin, extractives, and other chemicals such as mineral ions are lumped together as one component. This is a necessary and common simplification for this type of analysis.

Second, the method used here to determine FSP relies on calculating water chemical potential and EMC based on pore structure determined by MIP. Mercury intrusion measurements characterize the pore structure of wood in the dry non-swollen state, which may differ considerably from the pore structure when the cell wall is swollen, particularly in the region near the fiber saturation point. An alternative to MIP is the pressure plate or pressure membrane technique, which characterizes water in pores starting from a water-saturated state as discussed previously. Almeida et al. (2007) compared MIP and PPT measurements for seven hardwood species and found that, although the methods generally gave similar trends, EMC in the region near the fiber saturation point varied considerably between the two methods for certain species. However, the pressure membrane measurements of Zhang and Peralta (1999) and the here presented MIP measurements shown in Fig. 3 are fairly close in the moisture content range between 0.25 and 0.50 kg kg⁻¹. Furthermore, Zauer et al. (2014) found minimal differences in the pore size distributions determined by DSC of oven-dry Norway spruce versus the same material conditioned at 95 % RH.

Third, the analysis relies on extrapolation of desorption data and neglects sorption hysteresis. The method's accuracy is thus limited by the quality of the data and uncertainty regarding the extrapolation. In regard to sorption hysteresis, Le Maguer (1985) discussed the seeming paradox of using equilibrium thermodynamics to treat sorption data where there is more than one equilibrium state for a given chemical potential. He noted that both adsorption and desorption are equilibrium conditions; differences in moisture content between the two states arise from the fact that different states are available to the system in adsorption and desorption. The phase boundary could therefore be constructed from either adsorption or desorption data depending on which state was of interest.

Fourth, this analysis assumes that the sorption isotherm contains only bound water. The significance of pore water in the sorption isotherm has been widely

debated (Spalt 1958; Wangaard and Granados 1967; Simpson 1980; Skaar 1988; Engelund et al. 2010, 2013; Thygesen et al. 2010). In hardwoods, entrapped liquid water has been detected with NMR and magnetic resonance imaging (MRI) for samples that were conditioned in desorption from saturation at relative humidities as low as 76 % RH (Almeida et al. 2007; Passarini et al. 2014, 2015). In softwoods, Thygesen et al. examined whether capillary condensation (pore water) contributed to the sorption isotherm, and concluded that it was only appreciably contributing above 99.5 % RH for Norway spruce; in further work, they calculated its contribution as 0.35 % MC at 99.9 % RH based on geometrical arguments of an idealized softwood structure (Engelund et al. 2010; Thygesen et al. 2010). While a full analysis of the role of capillary condensation on the sorption isotherm is beyond the scope of the current paper, it appears that the implicit assumption of the framework presented in “[Extrapolation of the sorption isotherm](#)” section that the sorption isotherm contains only bound water is questionable at best and the results should be treated with caution.

Implications for wood–water interactions

The thermodynamic definition of the fiber saturation point presented in this paper (i.e., $\mu_{\text{H}_2\text{O}}^{\text{bound}} = \mu_{\text{H}_2\text{O}}^{\text{free}}$ at FSP) treats FSP as a thermodynamic phase boundary between bound and free water. This concept is now examined in light of other recent advances in understanding of the fiber saturation point (Babiak and Kudela 1995; Hill 2008; Engelund et al. 2010, 2013; Thygesen et al. 2010; Hoffmeyer et al. 2011; Derome et al. 2013).

The pressure plate/pressure membrane measurements and sorption isotherm measurements discussed above show continuity in equilibrium moisture content in the range of water activity from 0.96 to 0.98 (26–52 nm pore radius). This implies that bound water and free water exist in equilibrium in this range and that free water could be present at water activities less than 0.96. Free water could exist in microvoids and nanovoids within the wood structure at lower water activities, possibly as low as $a_w = 0.75$ (3.8 nm radius), as discussed by Thygesen et al. (2010). However, pressure plate measurements have not been published for wood at $a_w < 0.96$, to the best of the authors’ knowledge.

In theory, it is possible that DSC could be used to determine the phase boundary by detecting the phase transition of the first free water to melt (freeze). However, this technique is limited by noise; there needs to be enough free water freezing or melting to generate a signal. Alternatively, differences in nuclear magnetic resonance (NMR) measurements above and below the freezing point of water would indicate the presence of free water, again subject to the detection limit. While free water appears to be present at $a_w = 0.96$ based on the arguments above, the quantity may be undetectable. Thygesen et al. (2010) found a negligible difference in NMR signals for untreated Norway spruce sapwood at +20 and –20 °C.

Babiak and Kudela (1995) suggested replacing fiber saturation with two quantities: the “hygroscopic limit” which is similar to the traditional fiber saturation point where cell walls are filled with water, and an easily measurable

“cell wall saturation” based upon the difference in volume of the wood in smallest and most swollen state. Hill (2008) later noted that the method for calculating cell wall saturation is not strictly correct since it is calculated from external dimensions, which is not the same as the total change in cell wall volume. Instead, he suggested that fiber saturation not be used but instead “cell wall total capacity,” measured in solute exclusion measurements, be used to describe the true saturation of the cell wall.

Recent and important work by Engelund et al. (2013) carefully examined previous definitions of the fiber saturation point and the resulting implications for wood chemistry based upon the number of water molecules per free hydroxyl group in the wood. Instead of an exact definition of the fiber saturation point, they present the following continuum definition:

“Perhaps one should think of fibre saturation not as a state reached at a certain moisture content (i.e. a point) but as a gradual transition from the situation where new water molecules entering the cell wall result in breaking of intra- and intermolecular H-bonds in the wood cell polymers (i.e. up to about 30 % MC) to the situation (i.e. from about 30 to 40 % MC) where new water molecules are accommodated in the cell wall without breaking further cell wall polymer H-bonds.”

The most important aspect of the definition of Engelund et al. is that it addressed the traditional definition of Tiemann where the “free water has disappeared and the cell walls begin to [strengthen].” While researchers have been trying to attach a single numerical value to Tiemann’s theoretical definition for over 100 years, Engelund et al. have correctly pointed out that Tiemann’s definition encompasses several different phenomena that happen over a range of moisture contents. The physical properties appear to start changing (in desorption) at about 30 % moisture content. And at 40 % moisture content, there is clearly free water in pores of 0.4–1.5 μm (1–3.5 bar). The transition from 30 % MC to 40 % MC could be interpreted as free water filling the micropores within the wood structure.

Conclusion

The theoretical definition of fiber saturation was reviewed, and it was noted that methods used to determine the fiber saturation are in fact their own operational definition for measuring the fiber saturation. The theoretical definition forwarded in this paper, that the chemical potential of bound water is equivalent to the chemical potential of free water at FSP, is very similar to the concept of a thermodynamic phase boundary.

By defining fiber saturation as a phase boundary, it is a natural extension to develop a phase diagram or state diagram for the wood–water system. A preliminary state diagram was presented. The data exhibit a eutectic-like behavior which may give clues to the formation and interaction of free water in wood near the fiber saturation point. Further refinements of the state diagram may improve our understanding of moisture-induced durability failures in wood.

References

- Almeida G, Gagne S, Hernández R (2007) A NMR study of water distribution in hardwoods at several equilibrium moisture contents. *Wood Sci Technol* 41:293–307
- Anderson RB (1946) Modifications of the Brunauer, Emmett, and Teller Equation. *J Am Chem Soc* 68:686–691
- Araujo C, MacKay A, Hailey J, Whittall K, Le H (1992) Proton magnetic resonance techniques for characterization of water in wood: application to white spruce. *Wood Sci Technol* 26:101–113
- Babiak M, Kudela J (1995) A contribution to the definition of the fiber saturation point. *Wood Sci Technol* 29:217–226
- Berry SL, Roderick ML (2005) Plant–water relations and the fibre saturation point. *New Phytol* 168:25–37
- Choong ET, Tesoro FO (1989) Relationship of capillary pressure and water saturation in wood. *Wood Sci Technol* 23:139–150
- Cousins W (1976) Elastic modulus of lignin as related to moisture content. *Wood Sci Technol* 10:9–17
- Cousins W (1978) Young's modulus of hemicellulose as related to moisture content. *Wood Sci Technol* 12:161–167
- Dent RW (1977) A multilayer theory for gas sorption. Part I. Sorption of a single gas. *Text Res J* 47(2):145–152
- Deodhar S, Luner P (1980) Measurement of bound (nonfreezing) water by differential scanning calorimetry. In: ACS symposium series. American Chemical Society, Washington DC, pp 273–286
- Derome D et al (2013) The role of water in the behavior of wood. *J Building Phys* 36:398–421
- Engelund ET, Thygesen LG, Hoffmeyer P (2010) Water sorption in wood and modified wood at high values of relative humidity. Part 2: Appendix. Theoretical assessment of the amount of capillary water in wood microvoids. *Holzforschung* 64:325–330
- Engelund E, Thygesen L, Svensson S, Hill CS (2013) A critical discussion of the physics of wood–water interactions. *Wood Sci Technol* 47(1):141–161
- Feist WC, Tarkow H (1967) A new procedure for measuring fiber saturation points. *For Prod J* 17:65–68
- Flournoy DS, Kirk TK, Highley T (1991) Wood decay by brown-rot fungi: changes in pore structure and cell wall volume. *Holzforsch Int J Biol Chem Phys Technol Wood* 45:383–388
- Flournoy DS, Paul JA, Kirk TK, Highley T (1993) Changes in the size and volume of pores in sweetgum wood during simultaneous rot by *Phanerochaete chrysosporium* burds. *Holzforsch Int J Biol Chem Phys Technol Wood* 47:297–301
- Glass SV, Zelinka SL (2010) Moisture relations and physical properties of wood. In: Ross RJ (ed) *Wood handbook. Wood as an engineering material*. US Department of Agriculture, Forest Service, Forest Products Laboratory, Madison
- Glass SV, Zelinka SL, Johnson JA (2014) Investigation of historic equilibrium moisture content data from the Forest Products Laboratory. Forest Service, Forest Products Laboratory, General Technical Report, FPL-GTR-229, Madison
- Gliguem H et al (2009) Water behaviour in processed cheese spreads. *J Therm Anal Calorim* 98:73–82
- Griffin D (1977) Water potential and wood-decay fungi. *Annu Rev Phytopathol* 15:319–329
- Hailwood AJ, Horrobin S (1946) Absorption of water by polymers: analysis in terms of a simple model. *Trans Faraday Soc* 42:B084-B092-B084-B092
- Hatakeyama H, Hatakeyama T (1998) Interaction between water and hydrophilic polymers. *Themochimica Acta* 308:3–22
- Hernández R, Cáceres C (2010) Magnetic resonance microimaging of liquid water distribution in sugar maple wood below fiber saturation point. *Wood Fiber Sci* 42:259–272
- Hill CAS (2008) The reduction in the fibre saturation point of wood due to chemical modification using anhydride reagents: a reappraisal. *Holzforschung* 62:423–428
- Hill CA, Forster S, Farahani M, Hale M, Ormondroyd G, Williams G (2005) An investigation of cell wall micropore blocking as a possible mechanism for the decay resistance of anhydride modified wood. *Int Biodeterior Biodegradation* 55:69–76
- Hoffmeyer P, Engelund ET, Thygesen LG (2011) Equilibrium moisture content (EMC) in Norway spruce during the first and second desorptions. *Holzforschung* 65:875–882
- Jakes JE, Plaza N, Stone DS, Hunt CG, Glass SV, Zelinka SL (2013) Mechanism of transport through wood cell wall polymers. *J For Prod Ind* 2:10–13

- James WL (1963) Electric moisture meters for wood. US Forest Service Research Note FPL-08. US Forest Service Forest Products Laboratory, Madison
- James WL (1988) Electric moisture meters for wood. Forest Products Laboratory General Technical Report FPL-GTR-6. US Forest Service Forest Products Laboratory, Madison
- Kärenlampi PP, Tynjälä P, Ström P (2005) Phase transformations of wood cell water. *J Wood Sci* 51:118–123
- Lamason C, Macmillan B, Balcom B, Leblon B, Pirouz Z (2015) Water content measurement in black spruce and aspen sapwood with benchtop and portable magnetic resonance devices. *Wood Mat Sci Eng* 10:86–93
- Landry MR (2005) Thermoporometry by differential scanning calorimetry: experimental considerations and applications. *Thermochim Acta* 433:27–50
- Le Maguer M (1985) Solution thermodynamics and the starch-water system. In: Simatos D, Multon JL (eds) Properties of water in foods in relation to quality and stability. NATO ASI series. Series E. Applied Sciences; No. 90. Martinus Nijhoff Publishers in cooperation with NATO Scientific Affairs Division, Dordrecht/Boston/Lancaster
- Menon R, MacKay A, Hailey J, Bloom M, Burgess A, Swanson J (1987) An NMR determination of the physiological water distribution in wood during drying. *J Appl Polym Sci* 33:1141–1155
- Miki T, Sugimoto H, Kojiro K, Furuta Y, Kanayama K (2012) Thermal behaviors and transitions of wood detected by temperature-modulated differential scanning calorimetry. *J Wood Sci* 58:300–308
- Nakamura K, Hatakeyama T, Hatakeyama H (1981) Studies on bound water of cellulose by differential scanning calorimetry. *Text Res J* 51:607–613
- Olsson AM, Salmen L (2004a) The softening behavior of hemicelluloses related to moisture. ACS Publications, Washington DC, pp 184–197
- Olsson AM, Salmen L (2004b) The association of water to cellulose and hemicellulose in paper examined by FTIR spectroscopy. *Carbohydr Res* 339:813–818
- Passarini L, Malveau C, Hernandez RE (2014) Water state study of wood structure of four hardwoods below fiber saturation point with nuclear magnetic resonance. *Wood Fiber Sci* 46:480–488
- Passarini L, Malveau C, Hernández RE (2015) Distribution of the equilibrium moisture content in four hardwoods below fiber saturation point with magnetic resonance microimaging. *Wood Sci Technol* 49(6):1–18
- Repellin V, Guyonnet R (2005) Evaluation of heat-treated wood swelling by differential scanning calorimetry in relation to chemical composition. *Holzforschung* 59:28–34
- Roos Y, Karel M (1991a) Amorphous state and delayed ice formation in sucrose solutions. *Int J Food Sci Technol* 26:553–566
- Roos Y, Karel M (1991b) Applying state diagrams to food processing development. *Food Technol* 45(12):66, 68–71, 107
- Salmén L, Olsson A-M (1998) Interaction between hemicelluloses, lignin and cellulose: structure-property relationships. *J Pulp Pap Sci* 24:99–103
- Siau JF (1995) Wood: influence of moisture on physical properties. Department of Wood Science and Forest Products, Virginia Polytechnic Institute and State University Blacksburg, Virginia
- Simpson W (1980) Sorption theories applied to wood. *Wood Fiber Sci* 12:183–195
- Simpson LA, Barton AFM (1991) Determination of the fibre saturation point in whole wood using differential scanning calorimetry. *Wood Sci Technol* 25:301–308
- Skaar C (1988) Wood–water relations. Springer, New York
- Spalt H (1958) The fundamentals of water vapor sorption by wood. *For Prod J* 8:288–295
- Stamm AJ (1929) The fiber-saturation point of wood as obtained from electrical conductivity measurements. *Ind Eng Chem Anal Ed* 1:94–97
- Stamm AJ (1935) Shrinking and swelling of wood. *Ind Eng Chem* 27:401–406. doi:10.1021/ie50304a011
- Stamm AJ (1971) Review of nine methods for determining the fiber saturation points of wood and wood products. *Wood Sci* 4:114–128
- Stone JE, Scallan AM (1967) The effect of component removal upon the porous structure of the cell wall of wood. II. Swelling in water and the fiber saturation point. *Tappi* 50:496–501
- Telkki VV (2012) Wood characterization by NMR and MRI of fluids. *eMagRes* 1(1). doi:10.1002/9780470034590.emrstm1298
- Telkki V-V, Yliniemi M, Jokisaari J (2013) Moisture in softwoods: fiber saturation point, hydroxyl site content, and the amount of micropores as determined from NMR relaxation time distributions. *Holzforschung* 67:291–300

- Thygesen L, Elder T (2008) Moisture in untreated, acetylated, and furfurylated norway spruce studied during drying using time domain NMR1. *Wood Fiber Sci* 40:309–320
- Thygesen L, Elder T (2009) Moisture in untreated, acetylated, and furfurylated norway spruce monitored during drying below fiber saturation using time domain NMR. *Wood Fiber Sci* 41:194–200
- Thygesen LG, Tang Engelund E, Hoffmeyer P (2010) Water sorption in wood and modified wood at high values of relative humidity. Part I: results for untreated, acetylated, and furfurylated Norway spruce. *Holzforschung* 64:315–323
- Tiemann HD (1906) Effect of moisture upon the strength and stiffness of wood. US Department of Agriculture. Forest Service—Bulletin 70. Government Printing Office, Washington DC
- Trenard Y (1980) Comparaison et Interpretation de Courbes Obtenues par Porosimétrie au Mercure sur Diverses Essences de Bois. (Comparison and interpretation of Mercury Porosimeter curves obtained on some wood species). *Holzforschung* 34:139–146 (**In French**)
- Vuataz G (2002) The phase diagram of milk: a new tool for optimizing the drying process. *Lait* 82:485–500
- Wangaard FF, Granados LA (1967) The effect of extractives on water-vapor sorption by wood. *Wood Sci Technol* 1:253–277
- Weise U, Maloney T, Paulapuro H (1996) Quantification of water in different states of interaction with wood pulp fibres. *Cellulose* 3:189–202
- Zauer M, Kretzschmar J, Großmann L, Pfriem A, Wagenführ A (2014) Analysis of the pore-size distribution and fiber saturation point of native and thermally modified wood using differential scanning calorimetry. *Wood Sci Technol* 48:177–193
- Zelinka SL, Glass SV (2010) Water vapor sorption isotherms for southern pine treated with several waterborne preservatives. *ASTM J Test Eval* 38:80–88
- Zelinka SL, Lambrecht MJ, Glass SV, Wiedenhoeft AC, Yelle DJ (2012) Examination of water phase transitions in Loblolly pine and cell wall components by differential scanning calorimetry. *Thermochim Acta* 533:39–45
- Zelinka SL, Glass SV, Boardman CR, Derome D (2014) Moisture storage and transport properties of preservative treated and untreated southern pine wood. *Wood Mater Sci Eng*. doi:[10.1080/17480272.2014.973443](https://doi.org/10.1080/17480272.2014.973443)
- Zhang J, Peralta PN (1999) Moisture content-water potential characteristic curves for red oak and loblolly pine. *Wood Fiber Sci* 31:360–369